# Degree of synchronization of noisy maps on the circle

P. Khoury, M. A. Lieberman, and A. J. Lichtenberg
*Department of Electrical Engineering and Computer Sciences, and the Electronics Research Laboratory, University of California, Berkeley, California 94720*

(Received 11 January 1996; revised manuscript received 3 June 1996)

We consider two systems of nearly identical mappings on the circle, each having a single fixed point and additive noise. The noise moves each system between stable and unstable regions of the map, causing the separation of the systems to fluctuate. The geometric distribution of separations is characterized by a distribution exponent, which describes the degree of synchronization between the two systems. The distribution exponent is related to the conditional Lyapunov exponent, the more usual way of characterizing synchronization. The relation between the distribution and Lyapunov exponents is determined near the threshold of synchronization, where we prove that the two exponents change sign together. Fluctuations of separation that appear in systems driven by noise also appear in systems driven by chaos so that many of the methods may be useful for analyzing chaotic synchronization. [S1063-651X(96)02010-7]

PACS number(s): 05.45.+b, 02.50.Ey

## I. INTRODUCTION

Synchronization between the trajectories of two identical maps $w_{i+1}=h(\xi_i,w_i)$, $x_{i+1}=h(\xi_i,x_i)$, with different initial states, occurs when the separation between the two state variables at a particular iteration $|w_i-x_i|$ approaches zero for long times and for typical input $\xi$. If $\xi$ is chaotic the synchronization is known as chaotic synchronization. Pecora and Carroll first studied chaotic synchronization through use of a transmitting system and a subsystem of that transmitting system [1]. Later they generalized their approach to two systems fed with a chaotic input [2]. Their work is related to an earlier study which studies multiple mutually coupled chaotic systems [3]. Subsequently many papers have been published on the subject of chaotic synchronization [4–9]. Some of these have applied chaotic synchronization to the practical realm of secure communication [8,9]. If a receiver and transmitter behave chaotically and synchronize, information might be sent from one to the other with a low probability of intercept. Any practical system using chaotic synchronization, such as secure communication system, will be exposed to perturbations which might affect the synchronization of the system and thus the performance of the system. To choose the best operating parameters of systems used in applications, the degree of synchronization must be quantified. The quantification should be easy to measure and have clear physical meaning.

When the separation between the two systems is small, its evolution can be described using the instantaneous Lyapunov exponent of a single map. If the instantaneous Lyapunov exponent is positive the separation grows; if it is negative the separation shrinks. The greater the absolute value of the instantaneous Lyapunov exponent the greater the change in the separation for that mapping step. If the average of these instantaneous Lyapunov exponents approaches a positive value the two systems will be unsynchronized; if it approaches a negative value the two systems will be synchronized. The relation between this long term average, which we call the conditional Lyapunov exponent $\lambda$, and synchronization, was first noted by Pecora and Carroll [1,2]. When the driving signal $\xi$ is a noisy signal rather than a chaotic signal the instantaneous Lyapunov exponents are still well defined and retain the same physical significance. Thus systems with noisy inputs can also synchronize if the conditional Lyapunov exponent is negative.

Papers studying chaotic synchronization through computer simulations have described synchronization through the conditional Lyapunov exponent [1,2]. In a simulation the model is known and the conditional Lyapunov exponent can be easily calculated. However the Lyapunov exponent is difficult to measure experimentally, requiring considerable data and computation. In an experimental system other characteristics of synchronization may be easier to measure than the conditional Lyapunov exponent.

One easily measured characteristic of noisy and chaotic synchronization is the length of intermittent fluctuations of separation between two synchronizing systems. In the presence of either a chaotic or a noisy driving signal the instantaneous Lyapunov exponent fluctuates and may take on both positive and negative values. The fluctuations in an instantaneous Lyapunov exponent cause fluctuations of the separation between the two systems. The average separation, however, will have a drift which depends on the conditional Lyapunov exponent. If the conditional Lyapunov exponent is positive the average separation increases over time until the average separation is approximately the same as the system size. If the conditional Lyapunov exponent is negative, the average separation decreases over time, and if the two systems are perfectly identical the average separation will continue to shrink. However, if the two systems are slightly different or the driving signal sent to the two systems is slightly different (difference noise), the average separation will be asymptotically finite. Such differences are inevitable in any experimental system, as noted by researchers who have studied chaotic synchronization experimentally [2,10].

In an experimental system near the threshold of synchronization the fluctuations in separation are observed as intermittent bursts of synchronized behavior between two systems. The model for the evolution of the separation between two synchronizing systems is similar to the model for on-off

 

intermittency [11,12]. In a system driven by noise or chaos the on-off intermittency model predicts bursts of unsynchronized behavior interspersed with periods of synchronization and further predicts the scaling behavior of the probability of the bursts with the lengths of the bursts. This universal scaling behavior has been identified in the synchronized bursts of two chaotically synchronized systems [13]. The universal scaling behavior of on-off intermittency is easy to measure in the synchronized bursts of two systems; however, it only serves to identify synchronization behavior, not to quantify it.

In this paper we develop another tool for characterizing synchronization, the distribution exponent [14], which is a measurement made on two nearly identical maps. The degree of synchronization can be quantified by the distribution of the separations between the two systems; the distribution exponent describes this distribution and therefore has a strong connection to the intuitive notion of synchronization. We find that the probability distribution is geometric in separation (exponential in logarithmic separation) with parameter (exponent) $\sigma$, for separations lying between the magnitude of separations generated by the system differences and the magnitude of the system size. This exponent characterizes the degree of synchronization; it is negative if the two systems are synchronized and it is positive if the two systems are unsynchronized. We determine the distribution exponent and the connection between it and the conditional Lyapunov exponent. Pikovsky [14] introduced some of these ideas using a piecewise linear map on the circle [0,1) with uniform (large amplitude) additive noise, a case amenable to analysis. By examining the same map driven by arbitrary noise amplitudes we draw more general conclusions about the connections between the distribution and conditional Lyapunov exponents. We prove that the two exponents always have the same sign. For the piecewise linear map, we relate

$$\left.\frac{d\sigma}{d\lambda}\right|_{\lambda=0}$$

to the amplitude of the noise.

To measure the distribution exponent in any pair of systems, those systems must be nearly identical. If the differences between the systems are too large, no region exists having a probability of separation that scales geometrically. Generalized synchronization detects synchronization between two systems which have substantial differences by noting whether points close in the phase space of one system are also close in the phase space of the other system [15–17]. If the two systems are generally synchronized then there should exist a continuous map which takes points in one phase space to the other. From a set of data points from the two maps one determines the likelihood of the existence of a continuous map and thus the likelihood of synchronization. Further development of generalized synchronization to incorporate the distribution exponent is beyond the scope of this paper.

After formalizing the equations we use for study in Sec. II, we develop methods, in Sec. III, required to determine analytically the invariant distribution on the circle and use these to calculate the conditional Lyapunov exponent of a piecewise linear map over a range of additive noise amplitudes. This analysis is sufficiently general that it can be applied to other maps containing a single fixed point with additive noise on the circle. We then develop a formalism in Sec. IV to calculate the form of the invariant distribution of separation and its distribution exponent. For a piecewise linear map with additive noise, used as an example, we compare numerical and analytical results for the conditional Lyapunov exponent and obtain a correspondence between the conditional Lyapunov exponent and the distribution exponent at the threshold of synchronization. In the concluding discussion, in Sec. V, we show how these results concerning noisy synchronization might be generalized to apply to chaotic synchronization.

## II. FORMULATION IN SUM AND DIFFERENCE VARIABLES

The basic system used for analysis in this paper is two maps with additive noise

$$\begin{aligned} w_{n+1} &= h(w_n) + \theta_n, \\ x_{n+1} &= h(x_n) + \vartheta_n, \end{aligned} \tag{1}$$

for which the random processes $\theta$ and $\vartheta$ differ slightly as explained in the Introduction. These random processes can be split into a common component $\xi$ and an asymmetric component $\delta$,

$$\begin{aligned} \theta_n &= \xi_n + \frac{\delta_n}{2}, \\ \vartheta_n &= \xi_n - \frac{\delta_n}{2}. \end{aligned} \tag{2}$$

We use the expectation operator $\mathcal{E}$ [18] to measure the mean,

$$\mathcal{E}(x) = \int_{-\infty}^{\infty} x p(x) dx, \tag{3}$$

and the variance,

$$\mathcal{E}([x - \mathcal{E}(x)]^2) = \int_{-\infty}^{\infty} (x - \mathcal{E}(x))^2 p(x) dx, \tag{4}$$

of a random variable $x$, where $p(x)$ is the probability distribution function of $x$. In (2) the variance of the asymmetric component $\mathcal{E}([\delta - \mathcal{E}(\delta)]^2)$ is assumed to be orders of magnitude less than the variance of $\xi$ and therefore of the system variable $x$. Substituting (2) in (1) we obtain

$$\begin{aligned} w_{n+1} &= h(w_n) + \xi_n + \frac{\delta_n}{2}, \\ x_{n+1} &= h(x_n) + \xi_n - \frac{\delta_n}{2}. \end{aligned} \tag{5}$$

Equations (5) can be transformed by introducing the sum and difference variables

$$s_n=\frac{w_n+x_n}{2},$$
$$r_n=w_n-x_n. \tag{6}$$

The region where the invariant distribution of separation is geometric only occurs when $r$ is small. We limit our analysis to this region for which the expressions for $h(w)$ and $h(x)$ can be approximated by Taylor expansions

$$h(w_n)=h\left(s_n+\frac{r_n}{2}\right)\approx h(s_n)+h'(s_n)\,\frac{r_n}{2},$$
$$h(x_n)=h\left(s_n-\frac{r_n}{2}\right)\approx h(s_n)-h'(s_n)\,\frac{r_n}{2}. \tag{7}$$

Substituting (7) into (5) and adding and subtracting the two equations gives

$$s_{n+1}=h(s_n)+\xi_n, \tag{8}$$

$$r_{n+1}=h'(s_n)r_n+\delta_n. \tag{9}$$

The sum variable is now decoupled from the difference variable, and the difference variable depends in a simple way on the sum variable. The nonlinear terms, ignored in (7), keep $r$ bounded within the attractor size.

## III. DISTRIBUTIONS FOR THE SUM VARIABLES

### A. Linear map

We first examine (8) for linear maps $h(s)=ms+b$ with different types of additive noise $\xi$

$$s_{n+1}=ms_n+b+\xi_n. \tag{10}$$

The linear map (10) is unstable for $|m|>1$, with or without additive noise $\xi_n$. When $|m|>1$, a noise contribution increases with each iteration, and the variable $s$ does not remain bounded. We examine the case $|m|<1$ with white noise so that time steps are independent. Because the distribution of the sum of two independent random variables is the convolution of the two distributions, the convolution of the distribution of $h(s_n)$ with the distribution of $\xi$ gives the distribution of $s_{n+1}$. If the distribution $S$ of $s$ is to remain invariant it must satisfy the equation

$$S(s)=\frac{1}{m}\int_{-\infty}^{\infty}\Xi(s-s')S\left(\frac{s'-b}{m}\right)ds', \tag{11}$$

where $\Xi$ is the distribution of $\xi$, $m$ is the slope of the linear map, and $b$ is the intercept of the linear map.

The solution of (11) is straightforward if $\Xi$ is Gaussian. $S$ will be Gaussian because the convolution of two Gaussian distributions is Gaussian. To determine the entire distribution we determine its mean and variance which must remain the same before and after applying the map and adding the noise. For the mean

$$\mathcal{E}(s_{n+1})=\mathcal{E}(s_n), \tag{12}$$

and substituting (10) into (12) we have

$$\mathcal{E}(ms+b+\xi)=\mathcal{E}(s). \tag{13}$$

Decomposing the left hand side by using the linearity of the expectation operator, we obtain

$$m\mathcal{E}(s)+b+\mathcal{E}(\xi)=\mathcal{E}(s). \tag{14}$$

Solving for $\mathcal{E}(s)$ yields

$$\mathcal{E}(s)=\frac{\mathcal{E}(\xi)+b}{1-m}. \tag{15}$$

For the variance

$$\mathcal{E}([s_{n+1}-\mathcal{E}(s_{n+1})]^2)=\mathcal{E}([s_n-\mathcal{E}(s_n)]^2). \tag{16}$$

Substituting (10) into (16)

$$\mathcal{E}([ms+b+\xi-\mathcal{E}(s)]^2)=\mathcal{E}([s-\mathcal{E}(s)]^2), \tag{17}$$

using (15) in (17) and rearranging, we have

$$\mathcal{E}([ms-m\mathcal{E}(s)+\xi-\mathcal{E}(\xi)]^2)=\mathcal{E}([s-\mathcal{E}(s)]^2). \tag{18}$$

Using the independence of $s$ and $\xi$ to eliminate cross terms in the expectation on the left hand side of (18) and solving for $\mathcal{E}([s-\mathcal{E}(s)]^2)$, we have

$$\mathcal{E}([s-\mathcal{E}(s)]^2)=\frac{\mathcal{E}([\xi-\mathcal{E}(\xi)]^2)}{1-m^2}. \tag{19}$$

Note that the variance of the distribution $S$ is proportional to the variance of the noise distribution $\Xi$, and that the variance is singular at $m=\pm 1$. [Equations (12) through (19) apply to all distributions of the additive noise; however the invariant distribution of $s$ will not be the same as the distribution of $\xi$.]

### B. Nonlinear map

Self-consistency, developed in (12)–(19) to find the invariant distribution of a linear map can be used to find approximate invariant distributions of nonlinear maps. The technique works best on maps which transform a Gaussian distribution to a new distribution with a single maximum; we use such maps to illustrate the relation between the conditional Lyapunov and geometric exponents. When applied to maps with a single fixed point the approximation yields reasonable results. Multiple stable fixed points might be treated through rescaling techniques.

We approximate all distributions, before and after applying the mapping and the additive noise, with Gaussian distributions having the same mean and variance as the ones they approximate. Applying self-consistency by substituting (8) in (12), we have for the mean

$$\mathcal{E}[h(s)+\xi]=\mathcal{E}(s), \tag{20}$$

and substituting (8) in (16), we have for the variance

$$\mathcal{E}(\{h(s)+\xi-\mathcal{E}[h(s)+\xi]\}^2)=\mathcal{E}([s-\mathcal{E}(s)]^2). \tag{21}$$

Since $s$ and $\xi$ are independent (20) and (21) can be transformed to

$$\mathcal{E}[h(s)]+\mathcal{E}(\xi)=\mathcal{E}(s), \tag{22}$$

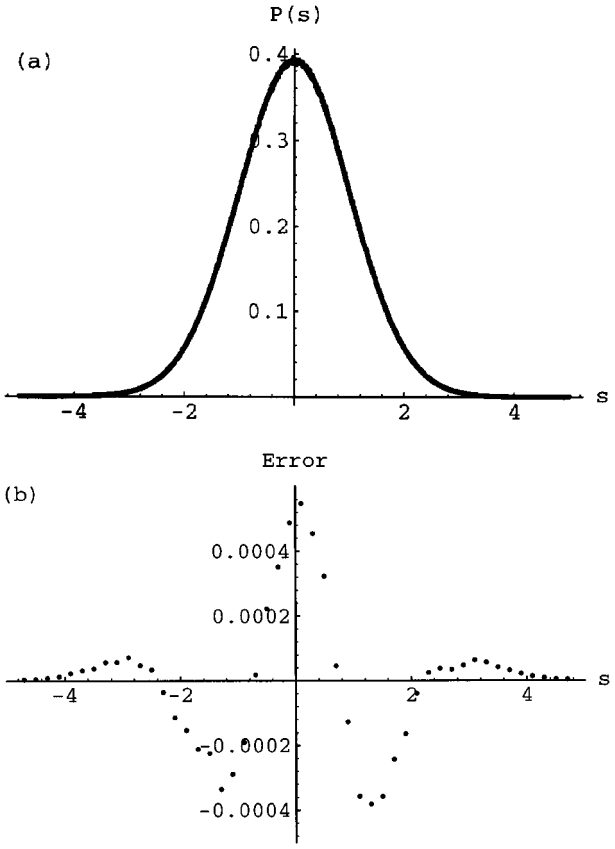


FIG. 1. (a) Invariant distribution of a piecewise linear map $h(x)$ with additive noise. The map is zero from $x=-1$ to $x=1$ and has slope 1/2 everywhere else. The noise is Gaussian white noise with unity variance. The computer simulation and the self-consistent prediction are indistinguishable from each other. (b) The error between a distribution estimated from a computer simulation of this map and a Gaussian distribution with mean and variance calculated using (22) and (23). The simulation was run through 50 000 000 iterations and sorted into overlapping bins of width $x=0.6$.

and

$$\mathcal{E}(\{h(s)-\mathcal{E}[h(s)]\}^2)+\mathcal{E}([\xi-\mathcal{E}(\xi)]^2)=\mathcal{E}([s-\mathcal{E}(s)]^2). \tag{23}$$

Assuming that $s$ is Gaussian with a given mean and variance we compute the new mean and variance of the transformed distribution $h(s)$. We verify the approximations by comparing the analytic results with computer simulations for a piecewise linear map which is 0 from $-1$ to 1 and has slope 1/2 everywhere else. The noise added to the map has mean 0 and unity variance. Numerical solution of (22) and (23) predict a mean of zero and a variance of 1.041. After a computer simulation of $5\times10^7$ iterations of the map, the variance is calculated to also be 1.041. Figure 1 shows the invariant distribution and the error between the Gaussian distribution with mean and variance calculated from (22) and (23) and the distribution determined from the computer simulation.

### C. Maps on the circle

To transfer the above results from the real line to the circle, the form of the noise must be adapted to the circle and new methods used to calculate the mean and variance. We transform Gaussian distributed noise on the real line to noise on the circle through use of a mod 1 mapping. In the limit of infinite variance on the real line the noise on the circle is uniformly distributed. As the variance of the noise distributed on the real line approaches zero, it and its transformation to the circle approach ''sure'' values equal to their means. Those means will be related by the mod 1 transformation.

We were able to use (3) to solve (13) and (20) because the sum of the mean of two independent random variables defined on the real line equals the mean of the sum of the same two random variables. However, the quantity defined by a truncated version of (3)

$$\int_{-1/2}^{1/2} xp(x)dx \tag{24}$$

does not have the distributive property for the addition of random variables on the circle. For this situation it is more useful to determine the mean from the derivative of the Fourier transform of $p(x)$ evaluated at zero frequency. For the mean on the real line we have

$$\mathcal{E}(x)=\int_{-\infty}^{\infty} xp(x)dx=i\,\frac{d}{d\omega}\int_{-\infty}^{\infty} e^{-i\omega x}p(x)dx\bigg|_{\omega=0}$$
$$=i\,\frac{d}{d\omega}P(\omega)\bigg|_{\omega=0}=\frac{d}{d\omega}\arg[P(\omega)]\bigg|_{\omega=0}. \tag{25}$$

Our definition for ''mean'' on a circle is the estimate of the derivative of the argument of the Fourier series at the origin from elements in the series. We use seven point formulas to estimate the derivative [19].

We define ''variance'' on the circle in a similar fashion; it is the estimate of the second derivative of the absolute value of the fourier series at the origin, which, on the real line, gives exactly

$$\mathcal{E}([x-\mathcal{E}(x)]^2)=-\left(\frac{d^2}{d\omega^2}P(\omega)-\left[\frac{d}{d\omega}P(\omega)\right]^2\right)\bigg|_{\omega=0}$$
$$=-\frac{d^2}{d\omega^2}\mathrm{Abs}[P(\omega)]\bigg|_{\omega=0}. \tag{26}$$

We compare simulated and analytical invariant distributions for two different maps; a continuous piecewise linear map, on $[-0.5, 0.5)$,

$$h(x)=\begin{cases} m_u x+\dfrac{m_u}{2}-\dfrac{1}{2}, & x<-\frac{1}{6} \\ m_s x, & -\frac{1}{6}\leqslant x<\frac{1}{6} \\ m_u x-\dfrac{m_u}{2}+\dfrac{1}{2}, & \frac{1}{6}\leqslant x \end{cases} \tag{27}$$

and the logistic map, on $[0,1)$,

$$h(x)=ax(1-x). \tag{28}$$

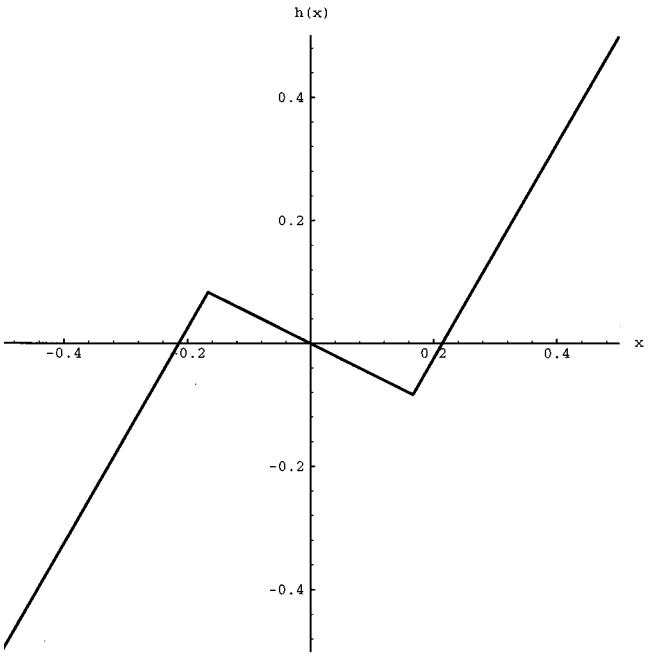


FIG. 2. A plot of the function $h$ in (27) with $m_s=-0.5$ and $m_u=1.75$.

For the piecewise linear map we take $m_s=-0.5$ as shown in Fig. 2. For the logistic map we take $a=2.5$. We add white noise $\xi_n$ to each map and take the result mod 1 to obtain the full system

$$x_{n+1}=[h(x_n)+\xi_n]\text{mod } 1. \tag{29}$$

Figure 3 compares the theoretical distributions from (22) and (23), using the approximations of (25) and (26), to find a mean and variance for the two maps (solid lines), with the computer simulations (dots) for $\mathcal{E}([\xi-\mathcal{E}(\xi)]^2)=0.02$.

## IV. DISTRIBUTIONS FOR THE DIFFERENCE VARIABLES

### A. Difference equation

Equation (9) describes the dynamics of the separation between the two subsystems. Following the work of Pikovsky [14], we consider a logarithmic transformation of (9),

$$z_n=\ln|r_n|, \tag{30}$$

without the difference noise $\delta$, to obtain

$$z_{n+1}=z_n+\ln|h'(s_n)|. \tag{31}$$

The quantity $\ln|h'(s_n)|$ is called the instantaneous Lyapunov exponent because it describes the change in the separation of two nearby maps over a single time step. The conditional Lyapunov exponent is the asymptotic average of the instantaneous Lyapunov exponents

$$\lambda=\lim_{N\to\infty}\frac{1}{N}\sum_{n=0}^{N}\ln|h'(s_n)| \tag{32}$$

over the orbit. It depends on the type of noise through the dependence of $s_n$ on the noise. We gather the instantaneous

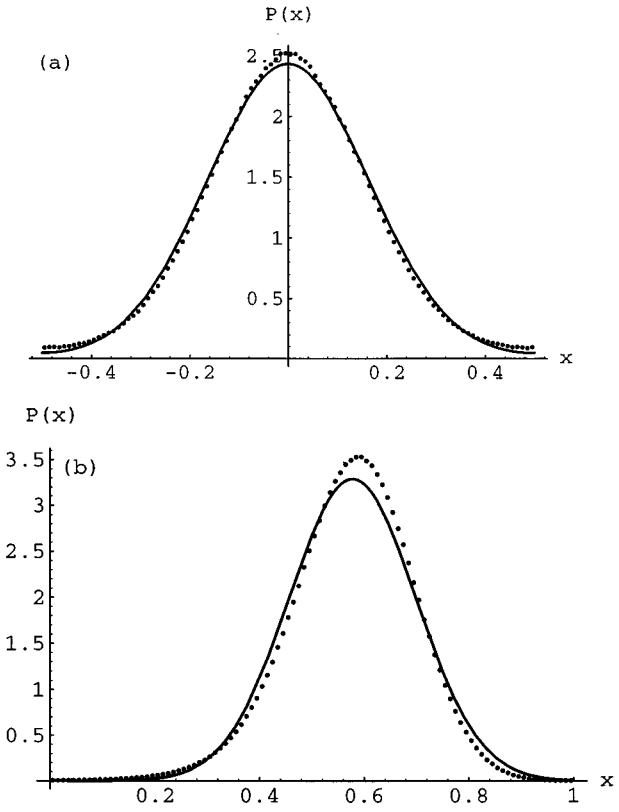


FIG. 3. (a) The invariant distribution of map (27) having parameter $m_s=-0.5$ with additive noise having variance 0.02. The points are generated from a simulation and the solid line is generated from (22) and (23) by using the procedures outlined in Sec. III C. (b) The invariant distribution of map (28) having parameter $a=2.5$ and added noise having variance 0.01. The points are generated from a simulation and the solid line is generated from (22) and (23) by using the procedures outlined in Sec. III C.

exponents together in groups of $N$ and average within those groups to determine a running average Lyapunov exponent (previously called a local Lyapunov in [14])

$$\Lambda_j^N=\frac{1}{N}\sum_{n=j}^{j+N-1}\ln|h'(s_n)|. \tag{33}$$

The evolution of the difference variable can be described using running average Lyapunov exponents, as

$$z_{N(i+1)}=z_{Ni}+N\Lambda_{Ni}^N. \tag{34}$$

We assume that adjacent running average Lyapunov exponents, $\Lambda_{Ni}^N$ and $\Lambda_{N(i+1)}^N$, become independent of each other as $N$ grows large because the correlation between adjacent running averages decreases as the group size grows. With this assumption their sum follows the central limit theorem. In addition we assume that $z$ and $\Lambda_{Ni}^N$ become independent for large $N$. In simulations we have found that the correlation between these two variables decreases as $N$ increases, justifying this assumption. Therefore an invariant distribution $Z(z)$ satisfies

$$Z_{N(i+1)}(z)=\int_{-\infty}^{\infty}L^N(\Lambda^N)Z_{Ni}(z-N\Lambda^N)d\Lambda^N, \tag{35}$$

where $L^N(\Lambda^N)$ is the invariant distribution of the running average Lyapunov exponents normalized such that

$$\int_{-\infty}^{\infty} L^N(\Lambda^N)d\Lambda^N = 1. \tag{36}$$

A form of $Z$ that satisfies this equation is

$$Z_{Ni}(z) = e^{\sigma z}. \tag{37}$$

Inserting (37) into (35) gives an expression for $\sigma$,

$$e^{\sigma z} = \int_{-\infty}^{\infty} L^N(\Lambda^N)e^{\sigma(z-N\Lambda^N)}d\Lambda^N, \tag{38}$$

or

$$1 = \int_{-\infty}^{\infty} L^N(\Lambda^N)e^{-\sigma N\Lambda^N}d\Lambda^N. \tag{39}$$

If $L^N(\Lambda^N)$ is known, then $\sigma$ can be calculated. Thus with these approximations, the invariant distribution for $z$ is exponential in $z$ with exponent $\sigma$. Transformation of this distribution to the separation $r$ gives a geometric distribution with parameter $\sigma$.

$$P(r) \propto r^{\sigma-1}.$$

To determine the number of solutions to (39) we define

$$S(\sigma) \equiv \int_{-\infty}^{\infty} L^N(\Lambda^N)e^{-\sigma N\Lambda^N}d\Lambda^N. \tag{40}$$

Solutions of (39) are solutions of

$$S(\sigma) = 1, \tag{41}$$

which depend on $L^N$ through the dependence of $S$ on $L^N$. We note that (41) has a trivial solution independent of $L^N$ by setting $\sigma = 0$ in (40). This yields

$$S(0) = \int_{-\infty}^{\infty} L^N(\Lambda^N)d\Lambda^N, \tag{42}$$

and by the normalization (36), we obtain

$$S(0) = 1. \tag{43}$$

Consider now the second derivative of (40)

$$\frac{d^2}{d\sigma^2} S(\sigma) = \int_{-\infty}^{\infty} N^2(\Lambda^N)^2 L^N(\Lambda^N)e^{-\sigma N\Lambda^N}d\Lambda^N. \tag{44}$$

Because every term in the integral in (44) is positive

$$\frac{d^2S}{d\sigma^2} > 0. \tag{45}$$

We use (43) and (45) to sketch $S(\sigma)$ in Fig. 4, showing all the ways that $S(\sigma)$ can cross the horizontal line $S=1$. We see that (41) has only one or two solutions. Because we expect the physical solution to depend on $L^N$ the trivial solution $\sigma = 0$ is ignored unless $S(\sigma)$ is a degenerate curve like the one in Fig. 4(c). The second solution corresponding to either Fig. 4(d) or 4(e) depends on $L^N$ and is the physical solution.

A difficulty with the exponential form is that it is not normalizable. However, we can impose cutoffs to remove the difficulty. For large differences the Taylor expansion in (7) fails; by physical reasoning the separation cannot grow beyond the attractor size, which is assumed to be bounded in $z$. At small scales the difference noise, ignored in (31), forces the two systems to remain separate.

If the system is more synchronized than not, the distribution exponent will be negative, and the two systems spend more of their time separated by small distances than by large ones. If the exponent is positive, the probability distribution will be weighted toward large separations. The larger the magnitude of the exponent the stronger the synchronization or desynchronization. The distribution exponent $\sigma$ is a continuous measure of the degree of synchronization that makes intuitive sense because it describes the probability of separation.

### B. An illustrative example

We use map (27) with additive noise to illustrate the ideas developed in Sec. IV A. We define two quantities $\lambda_s = \ln|m_s|$ and $\lambda_u = \ln|m_u|$. If we know the probability $p_s$ that the trajectory is in the stable region of the map and the probability $p_u$ that the trajectory is in the unstable region, we obtain the conditional Lyapunov exponent

$$\lambda = p_s\lambda_s + p_u\lambda_u. \tag{46}$$

From the invariant distribution, like the ones shown in Fig. 3(a) for a particular noise distribution we can determine the probabilities $p_s$ and $p_u$. Contour plots Figs. 5(a) and 5(b) compare the analytical results with simulation. The transition between synchronized and unsynchronized evolution of the two trajectories of a pair of maps (27) with additive noise occurs as the curve marked $\lambda = 0$ is crossed.

The distribution exponent is measured between trajectories evolving on two maps; for an invariant distribution of separations to exist the two maps must contain difference noise. We consider two copies of (27) with additive and difference noise

$$\begin{aligned} w_{n+1} &= \left( h(w_n) + \xi_n + \frac{\delta_n}{2} \right) \bmod 1, \\ x_{n+1} &= \left( h(x_n) + \xi_n - \frac{\delta_n}{2} \right) \bmod 1 \end{aligned} \tag{47}$$

for which the variance of $\delta$ is of order $10^{-12}$. Figure 6 gives three plots of the logarithm of the probability $P(z)$ versus the separation on the scale $z = \ln|r|$, for the three values of $m_s$ and common noise, given in the figure caption. The three cases correspond to strongly synchronized (steep negative slope), slightly synchronized, and unsynchronized (positive slope). The exponential behavior of the invariant distribution of separations is clear from the straight lines on the logarithmic plot. Below $z = -12$, the difference noise causes a dip in probability which destroys the exponential behavior. Above

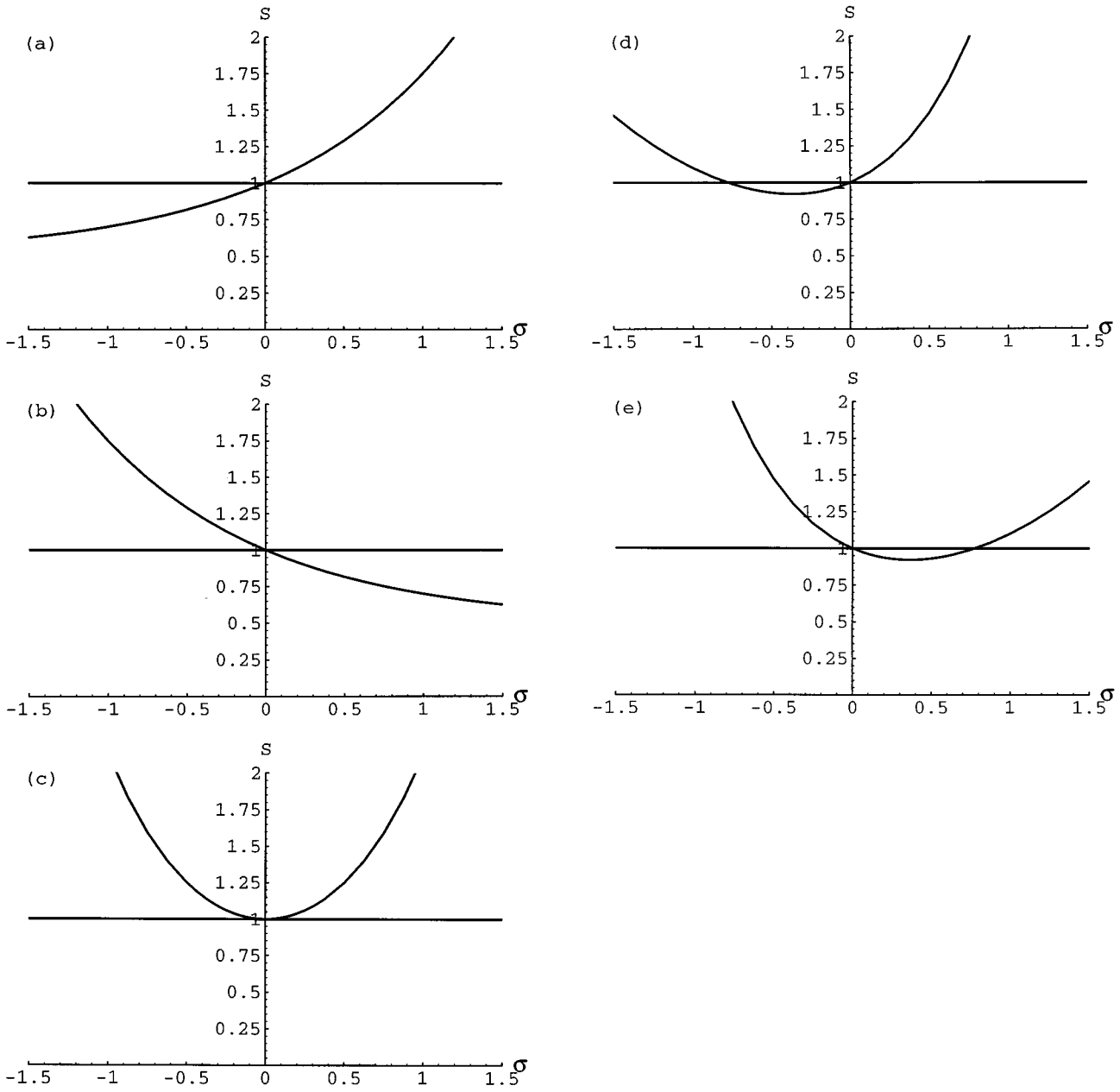


FIG. 4. Five different possible cases for the shape of the curve $S(\sigma)$ given in (40). Solutions to (41) appear as intersections between the curve and the line $s=1$, which is also plotted. In (a), (b), and (c) there is only one solution to (41) and the physical solution has gone to minus infinity, infinity, and zero, respectively; (d) and (e) each show two solutions to (41); the physical solution in (d) is negative while the physical solution in (e) is positive. Note that (c) is a degenerate case of (d) and (e).

$z=-7$ the Taylor expansion is not valid and the nonlinear terms bring the two subsystems closer to each other, keeping them within the attractor size.

Determining the behavior of the distribution exponent of the maps (47) can be easily done at the extremes of noise variance. Without noise the map is stable until the center slope $m_s$ drops below $-1$. Two identical stable maps without noise will stay synchronized and $\lim_{\delta\to 0}\sigma=-\infty$. When the fixed point goes unstable the whole map goes unstable, the two trajectories become completely unsynchronized, and $\sigma=\infty$. In the opposite extreme if uniform noise on the circle is added to the map at every iteration, the map is equally likely to visit any point on the interval $-1/2$ to $1/2$. This is the special case treated by Pikovsky [14]. At each step the map will be in the unstable region with probability $p_u=2/3$ and land in the stable region with probability $p_s=1/3$. This uniform noise forces independence between the current state of the system and any previous states such that, (39) holds exactly for $L^1$, from which we determine the distribution exponent analytically. The distribution of the running average for one time step is

$$L^1(\Lambda)=\tfrac{2}{3}\delta(\Lambda-\lambda_u)+\tfrac{1}{3}\delta(\Lambda-\lambda_s), \tag{48}$$

where here $\delta$ is the dirac $\delta$ function. Putting this into (39) gives an equation for $\sigma$

$$1=\tfrac{2}{3}e^{-\sigma\lambda_u}+\tfrac{1}{3}e^{-\sigma\lambda_s} \tag{49}$$

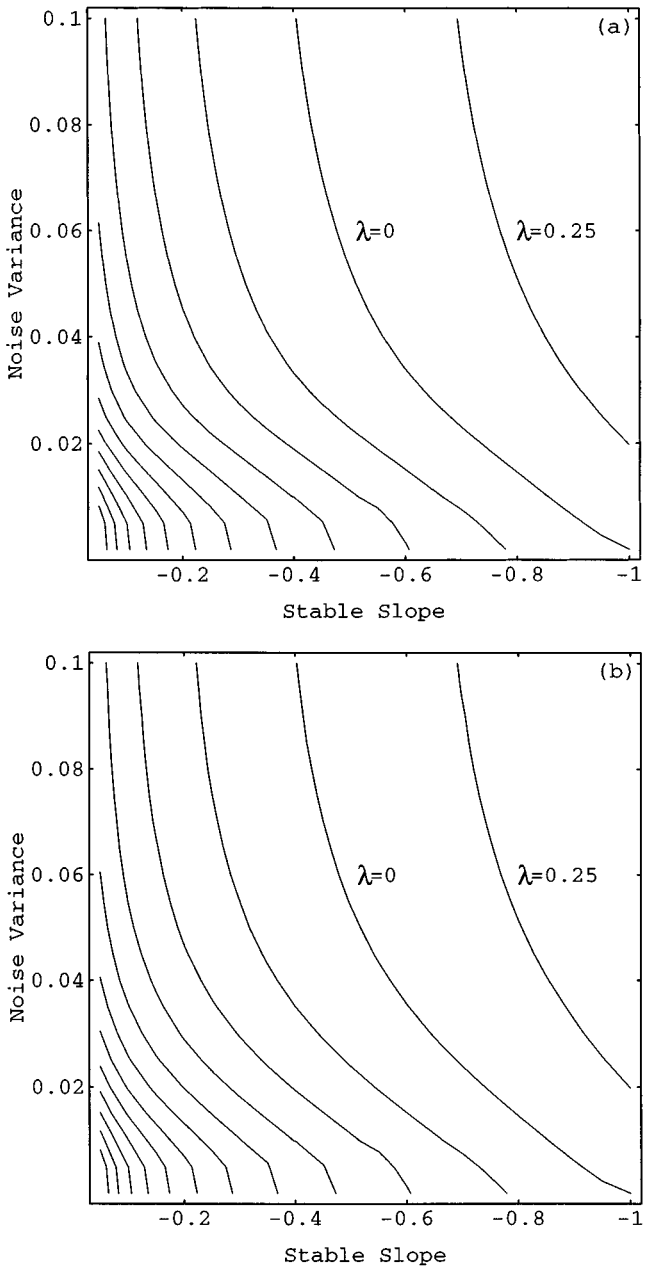


FIG. 5. Two contour plots of conditional Lyapunov exponent in the parameter space of noise variance $\xi$ and center slope $m_s$ of the piecewise linear map. The noise is Gaussian with a variance indicated on the vertical scale. The contour lines are spaced every 0.25. Plot (a) comes from analysis; plot (b), from simulation.

which can be solved numerically. Both $\sigma$ and $\lambda$ cross through zero when $m_s \approx -0.355$. If $m_s$ is less negative than this the two maps become synchronized and their trajectories stay close to each other despite the random fluctuations. If $m_s$ is more negative than $-0.355$, the trajectories of the two maps spend more time far apart in phase space than close to each other, i.e., the systems are unsynchronized. The distribution exponent characterizes the continuous transition between synchronized and unsynchronized behavior.

### C. Dependence between adjacent running averages

The maps of (47) can also elucidate the ideas of the running average Lyapunov exponent $\Lambda^N$ and the dependence between it and the separation $z$, an idea important in obtaining (35). The distribution exponent is much more difficult to determine analytically than the conditional Lyapunov exponent. Unlike the analysis leading to (49), we need to account for dependencies between time steps. As previously discussed, we average the instantaneous Lyapunov exponents over $N$ time steps such that the running average Lyapunov exponents $\Lambda^N$ become less dependent on each other. As $N$ increases in (39) its solution becomes a better approximation for $\sigma$.

The distribution of $\Lambda^N$ can be determined either through numerical simulation or through mapping of the invariant distribution. It is faster computationally to use numerical simulations. Figure 7 compares the predicted of the distribution exponent from (39) for a common noise variance of 0.0698 and $m_s=-0.1$ with increasing values of $N$, to the value of $\sigma$ measured from computer simulation (horizontal line). As $N$ increases the prediction becomes closer to the value measured in computer simulations, showing that the running averages become increasingly independent of the separation.

A main consequence of the dependence between instantaneous Lyapunov exponents is a modification of the variance. For the maps of (47) with a common noise level of 0.020 89 and a center slope $m_s=-0.5$ the probability of having $\Lambda^1=\lambda_s$ is 0.685 and the probability of having $\Lambda^1=\lambda_u$ is 0.315. A random variable created from an average of five samples of that random variable would have a variance of 0.0470. However the running average $\Lambda^5$ has a variance 0.0625. The variance of the running average is larger because after the instantaneous Lyapunov exponent has taken a value, either $\lambda_s$ or $\lambda_u$, it is more likely to take the same value during the next iteration.

### D. Normal distribution of running arverages

The distribution of $\Lambda^N$ for large $N$ approaches a normal distribution, a consequence of the ergodic theorem [20]. The mean of $\Lambda^N$ for large $N$ should be the same as $\Lambda^1$ and the variance of $\Lambda^N$ should decrease proportionally to $N$. Using a normal distribution in (39) gives

$$1=\int_{-\infty}^{\infty}\frac{1}{\sqrt{2\pi v/N}}\,e^{-(1/2)[(\Lambda-\lambda)^2/(v/N)]}e^{-N\sigma\Lambda}d\Lambda, \quad (50)$$

where the variance $v$ is

$$v=\lim_{N\to\infty} N\ \mathrm{var}(\Lambda^N). \quad (51)$$

The variance $v$ can be split into two pieces, the variance of the instantaneous Lyapunov exponent and the correction due to the dependency between time steps. The dependency correction is expressed through a diffusion coefficient [21]

$$D=\frac{1}{2}+\frac{\langle\Lambda_i^1\Lambda_{i+1}^1\rangle}{\langle(\Lambda_i^1)^2\rangle}+\frac{\langle\Lambda_i^1\Lambda_{i+2}^1\rangle}{\langle(\Lambda_i^1)^2\rangle}+\cdots \quad (52)$$

with $v$ expressed as

$$v=\mathcal{E}([\Lambda^1-\mathcal{E}(\Lambda^1)]^2)2D. \quad (53)$$

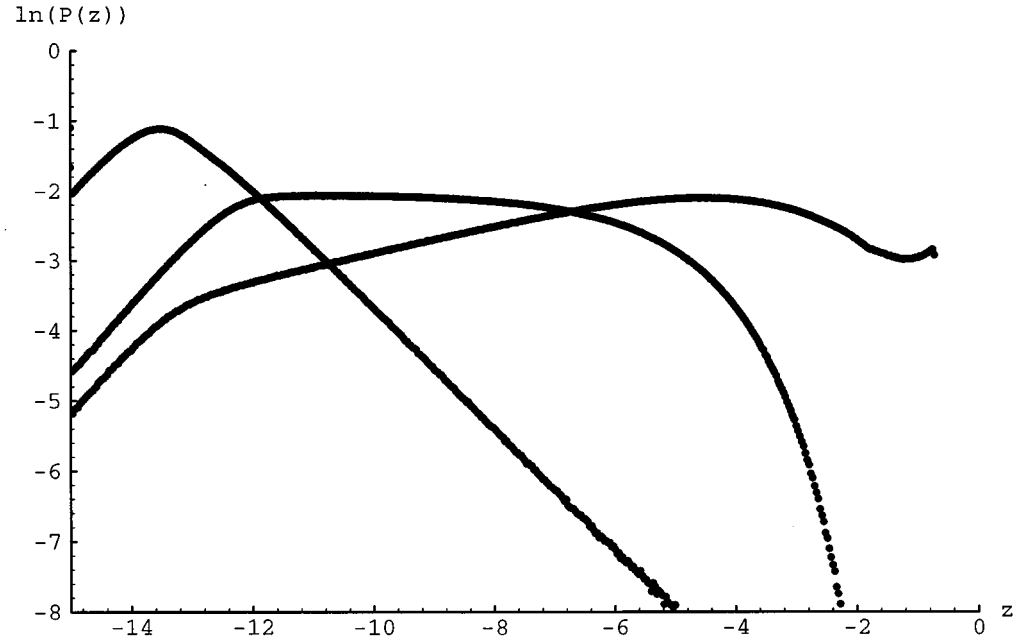


FIG. 6. $P(z)$, the probability density, is plotted on a logarithmic scale vs the separation $z=\ln|r|$. [$P(z)dz$ is the probability of finding the two systems described by the mapping (47) between the range of separations $z$ and $z+dz$.] The common noise is Gaussian. The difference noise is Gaussian with variance $10^{-12}$. There are three different maps shown. In the synchronized map $m_s=-0.1$ and common noise variance is 0.0698. The map that is barely synchronized has parameter $m_s=-0.951$ and common noise variance 0.002 31. The unsynchronized map has parameter $m_s=-0.5$ and common noise variance 0.0698.

Performing the integration in (50) we obtain

$$1=e^{-\lambda N\sigma+(1/2)(v/N)(N\sigma)^2} \tag{54}$$

and solving for $\sigma$ we find

$$N\sigma(\tfrac{1}{2}v\sigma-\lambda)=0. \tag{55}$$

Ignoring the trivial solution $\sigma=0$ we get

$$\sigma=\frac{2\lambda}{v}, \tag{56}$$

which is calculable from (32) and (51). The approximation of a normal distribution is best at the maximum of the Gaussian and deteriorates toward the tails. The further from zero $\lambda$ is, the more the tails are emphasized in the calculation for $\sigma$. Consequently the approximation holds best when $\lambda$ is close to zero.

### E. Relation between Lyapunov and distribution exponents

Figure 8 shows plots generated through computer simulation of $\sigma$ versus $\lambda$ for the maps of (47), with three different noise levels, obtained by varying $m_s$. Two features are clear from the plot. First $\sigma$ and $\lambda$ always change sign together; the graph stays in the first and third quadrants and always passes through the origin. This relationship can be proved for any distribution $L^N(\Lambda^N)$ through use of the properties of $S(\sigma)$. Recall that $S(0)=1$ and that $S$ always has positive curvature. The first derivative of $S$ is

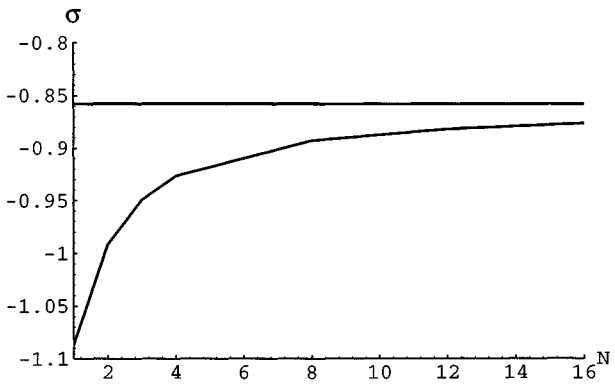


FIG. 7. Plot of the prediction for $\sigma$ produced by the distribution of $\Lambda^N$ for increasing $N$. The measurements were taken at a large noise level with a Gaussian variance of 0.069 and a center slope of the piecewise linear map of $-0.1$.

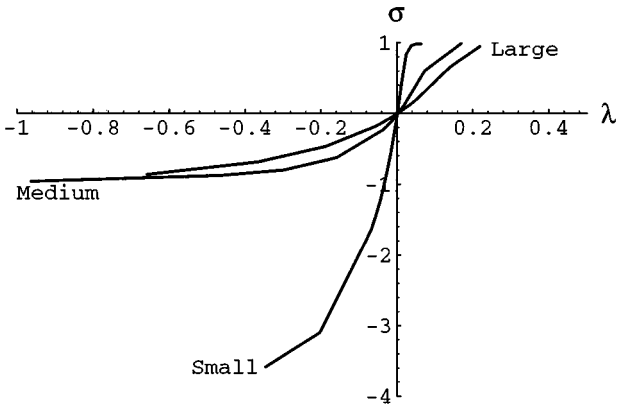


FIG. 8. Plot of the distribution exponent vs the Lyapunov exponent for three different noise levels. The large, medium, and low noise levels used had variances of 0.0698, 0.0209, and 0.002 315, respectively.

TABLE I. Comparison of the values of $d\sigma/d\lambda|_{\lambda=0}$ measured through computer simulations and predicted from Eq. (66) for various common noise variances. The diffusion coefficient was calculated through computer simulations.

| | Noise variance | Diffusion coefficient | $\left.\frac{d\sigma}{d\lambda}\right\|_{\lambda=0}$ Prediction | $\left.\frac{d\sigma}{d\lambda}\right\|_{\lambda=0}$ Simulations |
|---|---|---|---|---|
| Large noise | 0.069 773 | 1.269 | 3.64 | 3.53 |
| Medium noise | 0.020 895 | 1.415 | 7.27 | 7.08 |
| Low noise | 0.002 315 | 1.452 | 40.7 | 36.8 |

$$\frac{dS}{d\sigma}=-\int_{-\infty}^{\infty}N\Lambda^N L^N(\Lambda^N)e^{-\sigma N\Lambda^N}d\Lambda^N. \tag{57}$$

We evaluate (57) at $\sigma=0$ to obtain

$$\left.\frac{dS}{d\sigma}\right|_{\sigma=0}=-\int_{-\infty}^{\infty}N\Lambda^N L^N(\Lambda^N)d\Lambda^N. \tag{58}$$

Since, for any $N$,

$$\lambda=\int_{-\infty}^{\infty}\Lambda^N L^N(\Lambda^N)d\Lambda^N \tag{59}$$

we have

$$\left.\frac{dS}{d\sigma}\right|_{\sigma=0}=-N\lambda. \tag{60}$$

A negative Lyapunov exponent selects Figs. 4(a) and 4(d) as the only possibilities for the relationship between $S(\sigma)$ and the horizontal line $S=1$, because through Eq. (60) the slope of $S(\sigma)$ through $S(0)=0$ must be positive. So the second solution, if it exists, must be less than zero, as is the Lyapunov exponent. Similarly, if the Lyapunov exponent is positive, the slope must be negative, Figs. 4(b) and 4(e) are the only possibilities, and the second solution must be positive.

The second feature of Fig. 8 is that the transition through the origin is abrupt for low noise levels and gradual for large noise levels. The slope of the line at zero quantifies the rate of transition from synchronized to unsynchronized behavior. This slope can be determined analytically from (56). Using expressions for $\lambda$, $\Lambda^1$, and $v$

$$\lambda=p_u\lambda_u+p_s\lambda_s, \tag{61}$$

$$\langle(\Lambda^1)^2\rangle=p_u\lambda_u^2+p_s\lambda_s^2, \tag{62}$$

$$\begin{aligned}v&=\mathrm{var}(\Lambda^1)2D=[\langle(\Lambda^1)^2\rangle-\lambda^2]2D\\&=-(\lambda-\lambda_u)(\lambda-\lambda_s)2D,\end{aligned} \tag{63}$$

and substituting these into (56), we obtain

$$\sigma=\frac{-2\lambda}{(\lambda-\lambda_u)(\lambda-\lambda_s)2D}. \tag{64}$$

The derivative of (64) with respect to $\lambda$ is

$$\frac{d\sigma}{d\lambda}=\frac{2\left\{\lambda^2\left[1-\frac{d(\lambda_u+\lambda_s)}{d\lambda}\right]-\lambda_s\lambda_u+\lambda\lambda_u\frac{d\lambda_s}{d\lambda}+\lambda\lambda_s\frac{d\lambda_u}{d\lambda}\right\}}{(\lambda-\lambda_s)^2(\lambda-\lambda_u)^2 2D}. \tag{65}$$

Evaluating (65) at $\lambda=0$ yields

$$\left.\frac{d\sigma}{d\lambda}\right|_{\lambda=0}=\frac{-2}{\lambda_s\lambda_u 2D}. \tag{66}$$

where $\lambda_u$ and $\lambda_s$ take on values at $\lambda=0$ which depend on the noise level. Table I shows a comparison between measured values and predicted values of

$$\left.\frac{d\sigma}{d\lambda}\right|_{\lambda=0}.$$

The diffusion coefficient $D$ defined in (52) was calculated using computer simulations.

## V. CONCLUSIONS AND DISCUSSION

We have studied the synchronization of trajectories subject to difference noise through use of a piecewise linear map with additive white noise on the circle. To analyze the synchronization properties of the map we developed approximation methods to obtain the invariant distribution of maps with single fixed points on the circle. The invariant distribution can be used to determine the conditional Lyapunov exponent. We could easily measure and predict the conditional Lyapunov exponent because of our knowledge of the map used in the computer simulations. We developed another method of characterizing the degree of synchronization, using a distribution exponent. This exponent describes the invariant distribution of the separations between two nearly identical systems and is closely tied to the intuitive idea of synchronization. Using a pair of piecewise linear maps with difference noise, we obtained a distribution exponent describing the degree of synchronization between the maps. We also illustrated how dependence between time steps of the maps affects prediction of the distribution exponent. We related the distribution exponent to the conditional Lyapunov exponent near the threshold of synchronization, showing that they change sign together, and determining

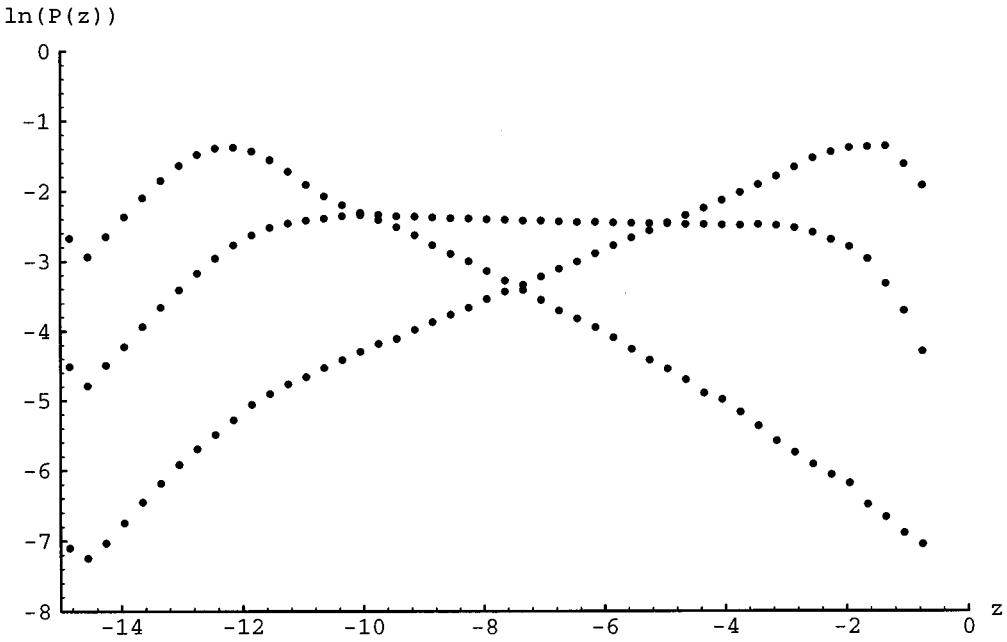


FIG. 9. Plot of probability of separation for two DPLL loops being fed by a common signal from another DPLL operating in the chaotic regime. $P(z)$ is plotted on a logarithmic scale versus $z=\ln|r|$.

$$\left.\frac{d\sigma}{d\lambda}\right|_{\lambda=0}.$$

The piecewise linear map driven by additive Gaussian white noise provides a basic system having both stable and unstable regions for determining the distribution exponent. However, maps that model many real systems are often driven by correlated noisy signals that are not Gaussian. We have observed exponential distribution of separation for the maps (47) with other forms of additive noise distributions, for the logistic map with additive Gaussian noise, for maps describing digital phase locked loops (DPLLs) [8] with random frequency input, and for DPLL systems that are fed not with noise but with a signal from a deterministic chaotic system.

The last case seems especially interesting since a chaotic input comes from a deterministic system and since different samples taken from a chaotic input signal are correlated. The correlation between samples taken of a chaotic input signal decreases as the time between the samples grows; however, the samples never become fully independent. Figure 9, which shows a graph remarkably similar to Fig. 6, was generated by a computer simulation of a DPLL system containing two nearly identical loops and fed with a signal from two other loops operating in the chaotic regime [8]. These loops were not fed by a random signal; i.e., the system is entirely deterministic. Yet Fig. 9 shows the same features as Fig. 6; an exponential distribution with a well defined slope and two cutoffs. Because of these results we suggest that the distribution exponent is well suited to measure chaotic synchronization.

## ACKNOWLEDGMENTS

We would like to acknowledge Maria de Sousa Vieira, who first brought Pikovsky's paper to our attention. This work was partially supported by ONR Grants N00014-95-I-0361 and N00014-89-J-1097, and by NSF Grant PHY-9505621.

[1] L. M. Pecora and T. L. Carroll, Phys. Rev. Lett. **64**, 821 (1990).
[2] L. M. Pecora and T. L. Carroll, Phys. Rev. A **44**, 2374 (1991).
[3] H. Fujisaka and T. Yamada, Prog. Theor. Phys. **69**, 32 (1983).
[4] A. Maritan and J. R. Banavar, Phys. Rev. Lett. **72**, 1451 (1994).
[5] A. Pikovsky, Phys. Rev. Lett. **73**, 2931 (1994).
[6] A. Maritan and J. R. Banavar, Phys. Rev. Lett. **73**, 2932 (1994).
[7] H. Herzel and J. Freund, Phys. Rev. E **52**, 3238 (1995).
[8] M. de Sousa Vieira *et al.*, Int. J. Bifurcation Chaos **2**, 645 (1992).
[9] U. Parlitz *et al.*, Int. J. Bifurcation Chaos **2**, 973 (1992).
[10] N. F. Rulkov and A. R. Volkovskii, in *Chaos in Communications (SPIE 2038) Proceedings, San Diego, CA, 1993* (SPIE, Bellingham, WA, 1993), pp. 132–140.
[11] P. W. Hammer *et al.*, Phys. Rev. Lett. **73**, 1095 (1994).
[12] N. Platt, E. A. Spiegel, and C. Tresser, Phys. Rev. Lett. **70**, 279 (1993).
[13] Y. H. Yu, K. Kwak, and T. K. Lim, Phys. Letters A **198**, 34 (1995).
[14] A. S. Pikovsky, Phys. Letters A **165**, 33 (1992).
[15] V. S. Afraimovich, N. N. Verichev, and M. I. Rabinovich, Izv. Vysch. Uchebn. Zaved. Radiofiz. **29**, 1050 (1986) [Sov. Ra-

diophys. **29**, 795 (1986)].
[16] N. F. Rulkov, M. M. Sushchik, L. S. Tsimring, and H. D. I. Abarbanel, Phys. Rev. E **51**, 980 (1995).
[17] L. M. Pecora, T. L. Carroll, and J. F. Heagy, Phys. Rev. E **52**, 3420 (1995).
[18] G. R. Grimmett and D. R. Stirzaker, *Probability and Random Processes* (Oxford University Press, New York, 1992).
[19] S. Yakowitz and F. Szidarovsky, *An Introduction to Numerical Computations* (Macmillan, New York, 1986).
[20] R. Durrett, *Probability: Theory and Examples* (Wadsworth Brooks/Cole, Pacific Grove, CA, 1991).
[21] H. Fujisaka, Prog. Theor. Phys. **70**, 1264 (1983).